

Single-shot fourth-order autocorrelator

Peng Wang,^{a,†} Xiong Shen,^{a,†} Jun Liu,^{a,b,c,*} and Ruxin Li^{a,b,c,*}

^aChinese Academy of Sciences, Shanghai Institute of Optics and Fine Mechanics, State Key Laboratory of High Field Laser Physics, Shanghai, China

^bUniversity of Chinese Academy of Sciences, Center of Materials Science and Optoelectronics Engineering, Beijing, China

^cChinese Academy of Sciences, Shanghai Institute of Optics and Fine Mechanics, CAS Center for Excellence in Ultra-intense Laser Science, Shanghai, China

Abstract. Temporal contrast (TC) is one of the most important parameters of an ultrahigh intense laser pulse. The third-order autocorrelator or cross correlator has been widely used in the past decades to characterize the TC of an ultraintense laser pulse. A novel and simple single-shot fourth-order autocorrelator (FOAC) to characterize the TC with higher time resolution and better pulse contrast fidelity in comparison to third-order correlators is proposed. The single-shot fourth-order autocorrelation consists of a frequency-degenerate four-wave mixing process and a sum-frequency mixing process. The proof-of-principle experiments show that a dynamic range of $\sim 10^{11}$ compared with the noise level, a time resolution of ~ 160 fs, and a time window of 65 ps can successfully be obtained using the single-shot FOAC, which is to-date the highest dynamic range with simultaneously high time resolution for single-shot TC measurement. Furthermore, the TC of a laser pulse from a petawatt laser system is successfully measured in single shot with a dynamic range of about 2×10^{10} and simultaneously a time resolution of 160 fs.

Keywords: ultrahigh intense laser; single shot; temporal contrast; four-wave mixing; fourth-order autocorrelator.

Received Jul. 1, 2019; accepted for publication Sep. 24, 2019; published online Oct. 23, 2019.

© The Authors. Published by SPIE and CLP under a Creative Commons Attribution 4.0 Unported License. Distribution or reproduction of this work in whole or in part requires full attribution of the original publication, including its DOI.

[DOI: [10.1117/1.AP.1.5.056001](https://doi.org/10.1117/1.AP.1.5.056001)]

1 Introduction

Many petawatt (PW) laser systems with the benefit of chirped pulse amplification (CPA)¹ and optical parametric CPA² techniques have been demonstrated in the past decade.³ State-of-the-art high-power laser systems can produce intense pulses with peak powers of 10 PW.⁴ In the future, laser systems may reach the 100-PW level⁵ with focal intensities of 10^{21} to 10^{24} W/cm².⁶ Ultrahigh intense laser pulses have been applied in the field of laser–matter interaction,⁷ such as proton or electron acceleration in thin solid targets^{8–10} and electron generation in fast-ignition inertial confinement fusion.^{11,12} For these applications, the temporal contrast (TC) of the ultraintense laser pulse is one of the most important parameters. Because the ionization threshold intensity of most solid targets is in the range of 10^{11} W/cm², the TC of ultraintense laser pulses should be higher than 10^{10} – 10^{13} to avoid damage to the target by the high-intensity background or prepulses. Recently, compressed

ultrahigh intense laser pulses with 10^{12} TC have been developed.¹³ Because most PW laser systems run at low repetition rates or even single shot, single-shot characterization of the TC of an ultraintense laser pulse is crucial.

Although many techniques have been developed to improve the TC of ultraintense laser pulses,^{14–16} only a few methods have been proposed for single-shot characterization of the TC. The first and most frequently used method for the measurement of the TC of single-shot pulses¹⁷ is third-order autocorrelator (TOAC). A time window of ~ 200 ps and a dynamic range of 10^6 were obtained using a pulse replicator in the TOAC.¹⁸ Using the optical parametric amplification process to generate the sampling pulse, a dynamic range as high as 10^{10} and a 50-ps time window with a 700-fs time resolution were achieved by Qian's group based on a fiber-array-based detection system.¹⁹ With typical TOAC and third-order cross correlator (TOCC) processes, it is hard to achieve single-shot pulses with simultaneous high dynamic range, precise time resolution, high-pulse contrast fidelity, and wide time window, which are the most important parameters for TC characterization. Recently, the SRSI-ETE method was demonstrated, which has a time resolution as high as 20 fs.^{20–22} However, the dynamic range is limited by the

*Address all correspondence to Jun Liu, E-mail: jliu@siom.ac.cn; Ruxin Li, E-mail: ruxinli@mail.siom.ac.cn

[†]These authors contributed equally to this work.

signal-to-noise ratio of the detector and, at present, the highest achievable value is 10^8 . Together with the TC reduction method, 10^9 dynamic range has recently been obtained using SRSI-ETE.²³

In this paper, we propose a single-shot measurement method named “fourth-order autocorrelation” for the single-shot TC characterization of ultraintense laser pulses. In this method, frequency-degenerate third-order nonlinear processes, such as cross polarization wave generation (XPW),^{16,24} self-diffraction (SD),^{25,26} and transient grating (TG),²⁷ have the potential to generate cleaner signal pulses, which can then be used as the cleaning reference (or sampling) pulses for the next sum-frequency mixing (SFM) process together with the test pulse. In the proof-of-principle experiment, the SD process is used to generate the cleaning sampling pulse in the single-shot fourth-order autocorrelator (FOAC). A single-shot measurement with 10^{11} dynamic range, 65-ps time window, and 160-fs time resolution has been achieved.

Compared with previous single-shot TOAC or TOCC methods, the single-shot FOAC has the following advantages. First, cleaner sampling pulses are generated by the third-order nonlinear processes and, as a result, higher fidelity measurement is achieved. Second, the closeness of the sampling pulse and test pulse central wavelengths results in a high time resolution for the single-shot measurement, owing to the neglecting influence of the group velocity mismatch (GVM) during the SFM process. Third, hundreds of microjoule sampling pulses are generated by a simple SD process, and a 10^{11} dynamic range is achieved. Furthermore, two improvements are made in the proof-of-principle experiment to reduce the noise and extend the time window. First, the beta-barium borate (BBO) crystal for SFM is cut with a large angle to reduce the noise from the second-harmonic generation (SHG) signals of both the sampling pulse and test pulse. Second, the aperture of the BBO crystal for SFM is extended to a width of 21 mm, which can support a 65-ps time window in single-shot measurement.

2 Principle of Fourth-Order Autocorrelation

To further explain the principle of fourth-order autocorrelation, we will compare it with second- and third-order correlations, which are used in the characterization of pulse duration and TC, respectively. In the second-order autocorrelation, the ultrashort pulse to be measured, which is shown in Fig. 1(a), is used as its own sampling pulse by splitting the pulse into two replicas $I(t)$ and $I(t - \tau)$. As a result, the corresponding autocorrelation signal is given by

$$S_2(\tau) = \int_{-\infty}^{\infty} I(t)I(t - \tau)dt, \quad (1)$$

where τ is the relative time delay. Then second-order autocorrelation signal is always symmetric in time, and asymmetric pulses cannot be recognized by second-order autocorrelation, as shown in Fig. 1(b).

To measure an asymmetric pulse shape and the TC of an ultraintense laser pulse, third-order autocorrelation was proposed in 1993.¹⁷ First, the sampling pulse is obtained using the typical SHG of the test pulse. Then it is followed by a frequency nondegenerate SFM process, which is also a second-order nonlinear process. The corresponding signal can be expressed as

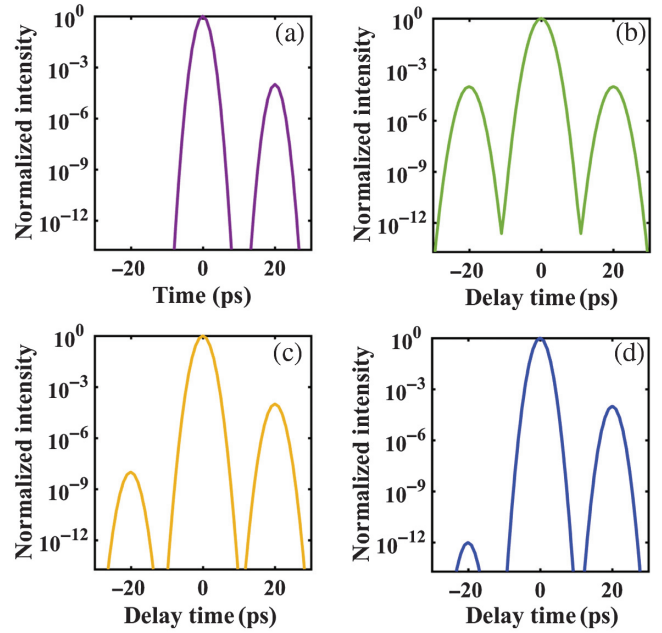


Fig. 1 (a) The testing pulse with a postpulse, (b) the second-order autocorrelation signal, (c) the third-order autocorrelation signal, and (d) the fourth-order autocorrelation signal.

$$S_3(\tau) = \int_{-\infty}^{\infty} I^2(t)I(t - \tau)dt, \quad (2)$$

where τ is the relative time delay. Obviously, third-order autocorrelation signal $S_3(\tau)$ is asymmetric, and the prepulses and postpulses can be distinguished clearly, as shown in Fig. 1(c). At present, commercial TOACs based on delay-scanning optical setups can guarantee a 10^{10} dynamic range capability. With the usage of noise filtering, a high-sensitivity detector, and an attenuator, dynamic ranges as high as 10^{13} can be achieved using delay-scanning TOAC.²⁸ Because the wavelength of the third-order autocorrelation signal is different from those of the SHG signals of the two incident pulses, it can suppress the scattering noise from the two incident pulses using a spectral filter, which leads to a high dynamic range. However, two problems persist. First, the time resolutions of the delay-scanning TOACs are limited to about 250 fs, according to previous works,^{19,20} mainly due to the GVM induced by the large central wavelength difference between the sampling pulse and the test pulse and the thickness of the nonlinear crystal. Second, strong postpulses will still induce ghost prepulses in the third-order correlation signal, as shown in Fig. 1(c). As the dynamic range of TC increases, the ghost prepulses become detectable, which will affect the fidelity of the measurement.

To solve these two problems, fourth-order autocorrelation is proposed here. In the fourth-order autocorrelation, the sampling pulse is generated by frequency-degenerate four-wave mixing processes, such as SD, XPW, and TG, which are third-order nonlinear processes. Then the fourth-order autocorrelation signal is obtained by the following SFM process. As a result, a third-order nonlinear process and a second-order nonlinear process make up the fourth-order autocorrelation, which can be expressed as

of the correlation signal, a strip-shaped density filter, with an approximately four orders of magnitude attenuation of the main pulse, and a coated wedge that introduces an attenuated reference replica signal below the original correlation signal are placed behind the BBO crystal. The strip-shaped density filter with a metallic coating has a fixed attenuation ratio about 10^4 for the SFM signal around 400 nm, which has been calibrated before the experiment. The coated wedge would introduce a reference replica signal with about 70 times attenuation due to the back-and-front reflection on the surface of the wedge. Because of the diffraction, the edge effect would influence the signal near the edge of the strip-shaped density filter. However, the density filter is placed right behind the BBO crystal and the correlation signal is imaged from the BBO crystal to the sCMOS sensor by a 4f imaging system. By carefully adjusting the 4f imaging system, the influence of the diffraction effect would be weakened. A bandpass filter with a central wavelength of 400 nm is placed in front of the sCMOS camera to avoid noise from the fundamental incident pulses. The whole setup is compact and economical as a single-shot measurement apparatus.

5 Experimental Results and Discussion

A femtosecond Ti:sapphire regenerative amplifier (8 mJ/1 kHz/40 fs) is used to test the fourth-order autocorrelation method and the single-shot FOAC device at first. A high autocorrelation signal means a high dynamic range of the single-shot measurement. Considering the low-energy transfer efficiency of the SD process, laser pulses of ~ 8 mJ with a diameter of about 10 mm are all guided into the experimental setup. After the first beam splitter, the 2-mJ laser pulse is used as the test pulse and the left 6-mJ is used for sampling pulse generation. Intense SD sidebands are generated when the two input beams intersect each other with a 1.3-deg angle in air and synchronously overlap in both time and space. The pulse energy of the first-order SD signal is measured to be $150 \mu\text{J}$ with an efficiency of 2.5%, which can support a high dynamic range single-shot TC measurement. The generated SD signal has a smoother spectrum and cleaner TC than the input pulses. More details about the generation of the sampling pulse based on the SD process can be found in our previous paper.²⁵

The sampling and test pulses are then focused onto a large wedge-designed BBO crystal. The BBO has a central thickness of 1.5 mm to increase the intensity of the correlation signal and to improve the measurable dynamic range at the expense of decreased phase-matching bandwidth. By capturing the spectrum of the sum frequency generation (SFG) signal, the bandwidth of the SFG process is estimated to be about 20 nm. If the test pulse has a broadband spectrum, the phase-matching bandwidth may not be broad enough to cover the whole spectrum in the SFG process with a thicker nonlinear crystal. Fortunately, the spectral bandwidths of the main pulse, the pre- or postpulses, and the ASE background or fluorescence noise usually have the same spectral bandwidth, and the SFG signal intensities of their responses to the phase-matching bandwidth narrowing during SFG process are equal. Then the generated SFG signal with a narrow bandwidth using a thicker nonlinear crystal would have negligible influence on the TC ratio. Because the time window is determined by the crossing angle and the diameter of the BBO, the BBO is designed to have a large aperture of 21 mm and a cutting angle of 80 deg, which supports the phase-matching angle of 32 deg in the crystal. Furthermore,

in the experiment, the relatively large cutting angle reduces the noise from SHG signals of both sampling and test pulses.

By adjusting the time delay between the sampling and test pulses, the autocorrelation signal of the main pulse can be observed as a bright blue spot on a white paper. The bright blue spot moves along the horizontal direction as the time delay changes. This is because the overlapping zone between the sampling and main pulses of the test pulse changes continuously with the time delay. The intense correlation signal guarantees a high dynamic range of the measurement, which has to be preprocessed due to the limited dynamic range of the sCMOS camera. Several steps are involved in obtaining a high dynamic range TC measurement. First, the correlation signal from the main pulse of the test pulse is so intense that a strip-shaped density filter is added after the BBO crystal to attenuate the intensity of the main pulse directly. However, some strong prepulses or postpulses can still saturate sCMOS camera. In that case, a coated wedge is added, which will introduce a reference replica signal with about 70 times the attenuation in the shifted area of the sCMOS sensor. As a result, the original authentic intensity of the saturated main pulse and strong satellite pulses can be retrieved with the reference replica. Finally, the autocorrelation signal passes through a bandpass filter and is sent into the sCMOS.

Figure 4(a) shows the fourth-order autocorrelation signal obtained using the sCMOS camera when the exposure time is 1 ms. The intense signal is the original autocorrelation signal of which the strongest signal from the main pulse has already been attenuated by a strip-shaped density filter. The weaker signal line below without saturation is the attenuated replica

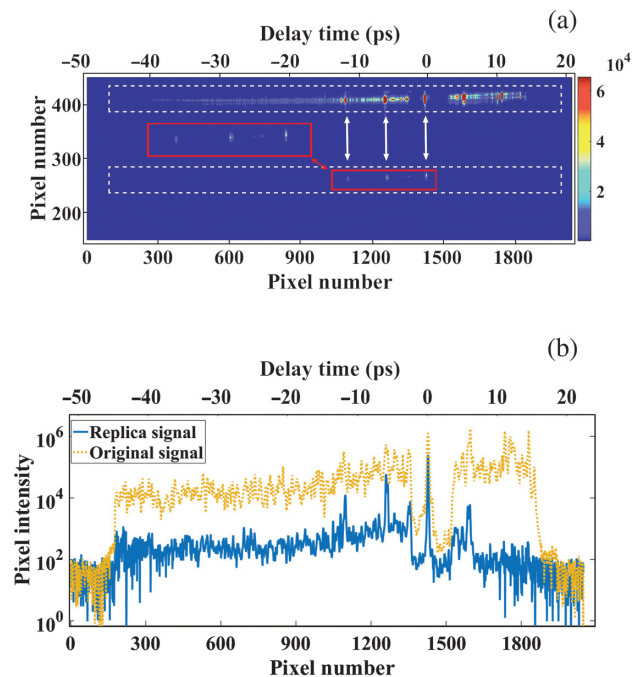


Fig. 4 (a) The intensity distribution of the original signal and the replica on the sCMOS. The original signal and the replica are shown in the rectangle area marked with white-dashed lines. The part of the replica signal marked with red lines is zoomed for better visibility in the larger of the two red rectangles. (b) The intensity distribution of the original signal and the replica along the horizontal direction.

signal introduced by the front-and-back reflection of the coated wedge, which can be used to obtain the original real intensity of the main pulse and the strong postpulses or prepulses.

The bright correlation signal detected by the sCMOS camera covers an area of $\sim 20 \times 1770$ pixels in the vertical and horizontal directions, respectively, where the time window is encoded into the horizontal direction. The time window can be calculated by $2 \times l \times p \times \sin(\theta)/c$, where l is the pixel size of the sCMOS sensor, p is the pixel number relative to the center of the main pulse, θ is the crossing angle of the sampling pulse and the autocorrelation signal in air, and c is the speed of light in air. As a result, the time window is ~ 65 ps in this experiment and each $11\text{-}\mu\text{m}$ pixel corresponds to ~ 37 fs. After summing up the intensity of the 20 pixels along the vertical direction and subtracting the background noise of the sCMOS, the intensity profile along the horizontal direction is obtained, as shown in Fig. 4(b). Obviously, pixel numbers between 1372 and 1516 or delay times between -2 and 3.2 ps are attenuated by the strip-shaped density filter. In the vertical direction, all the 20 pixels for the main pulse are all saturated of the original SFG signal. However, for those prepulses or postpulses in the original SFG signal, only a few pixels get saturated as shown in Fig. 4(a), but not all the 20 pixels are saturated. Therefore, even though the main pulse shows a saturation peak, the pre and postpulses do not have the same peak level, as shown in Fig. 4(b). The same method is used to process the data of the replica signal in Fig. 4(a), and the intensity profile of the weaker replica signal is obtained as shown in Fig. 4(b) (blue solid line). Thus the intensity of the saturated correlation peaks can be retrieved correctly.

The real intensity of the main pulse is obtained by multiplying the attenuation ratio of the strip-shaped density filter and the front-and-back reflection of the coated wedge. Furthermore, two shots of FOAC with shifted times are measured and combined together to further extend the time window. The final TC profile measured by the novel FOAC is shown in Fig. 5 (dotted line). The TC of the kHz laser pulses has a dynamic range of 10^8 , and the time window with two shots is extended to ~ 106 ps with 48 and 58 ps in the front and back edges, respectively. The 10^{10} dynamic range at both ends of time window shows the background of sCMOS without correlation signal, which indicates good capability of the dynamic range measurement. To confirm the reliability of the FOAC results, the TC of the test pulse is also measured using a commercial delay scanning TOAC (Amplitude Technologies Inc., Sequoia-800). Obviously, both the experimental results are in good accordance with each other except for one prepulse at -30 ps with $\sim 10^{-4}$ intensity,

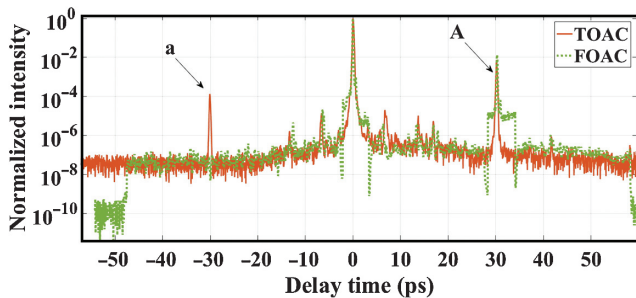


Fig. 5 TC results of a Ti:sapphire regenerative amplifier measured using the Sequoia-800 (solid line) and our single-shot FOAC equipment (dashed line).

labeled as “a,” which only appeared in the measurement profile using the Sequoia-800. Furthermore, we found a stronger postpulse at the mirror delay time of 30 ps with $\sim 0.7 \times 10^{-2}$ intensity, which is labeled as “A.” This means that the prepulse “a” is a ghost pulse introduced by postpulse “A” during the TOAC measurement by the Sequoia-800. It should be noted that the ghost prepulse “a” is not detected by the proposed single-shot FOAC, which shows much higher measurement fidelity than TOAC. As previously mentioned, this is because the sampling pulse of our single-shot FOAC is generated by a third-order nonlinear process, which has a cleaner TC compared with the sampling pulse generated by SHG in the Sequoia-800 based on TOAC.

The time resolution is another important parameter in TC measurement. Although the time step can be as short as 10 fs, the time resolution of a delay-scanning TOAC is limited to hundreds femtoseconds by the large GVM between the test pulse and its SHG sampling pulse. In all previous works, the time resolution of single-shot TOAC or TOCC measurements was always wider than 500 fs due to GVM and the limitation of detectors. Because the sampling pulse has the same central wavelength as the test pulse in this single-shot FOAC, the GVM is not a problem. Ideally, a time resolution of ~ 37 fs can be obtained when considering an $11 \mu\text{m} \times 11 \mu\text{m}$ pixel size. The spatial resolution of the 1:1 4f imaging system, which is used to map the correlation signal from the SFM crystal to the sCMOS sensor, limits the time resolution of this proof-of-principle experiment to ~ 160 fs. By enlarging the main peak pulse in Fig. 5 with a linear intensity scale, the correlation profiles by the Sequoia-800 and by single-shot FOAC are shown in Fig. 6, where the pulse duration of the test pulse is ~ 40 fs. A high spatial resolution of the 1:1 4f imaging system with a shorter focal length or larger NA is expected to improve the time resolution of this FOAC. A magnified 4f imaging system can also improve the time resolution; however, the time window will be narrowed at the same time. A wider time window can be obtained with a reduced 4f imaging system and a larger camera sensor.

To further test the dynamic range capability of our method, we also measured the TC of another laser system using the single-shot FOAC, in which the laser pulse with the parameters of 20 mJ/10 Hz/40 fs/800 nm is used in the experiment. In comparison to the kHz system, both the obtained SD signal and the test pulse have higher pulse energies of $450 \mu\text{J}$ and 4 mJ, respectively. As a result, a higher SFM signal can be obtained, which makes it possible to further enhance the dynamic range. The original correlation signal obtained by the

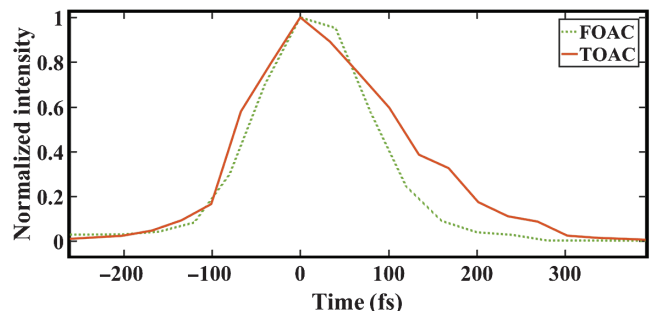


Fig. 6 Correlation traces by the TOAC and FOAC with a linear plot of intensity.

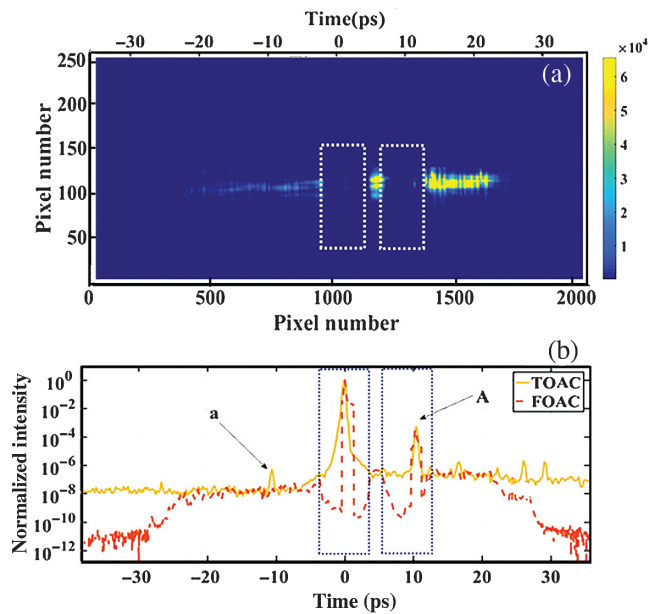


Fig. 7 The measurement results with a dynamic range of 10^{11} by the FOAC. (a) The correlation signals on the sCMOS detector. (b) The comparison of the TOAC and FOAC measurement results. The strip-shaped density filters are used in the region of the dashed-line rectangle.

sCMOS is shown in Fig. 7(a), where two strip-shaped density filters are used to attenuate the main peak signal. A 1-mm glass plate is used to introduce a postpulse for the test pulse, the signal of which is also attenuated by a strip-shaped density filter. The coated wedge is unnecessary in this measurement. Figure 7(b) shows the retrieved TC curves obtained by both the single-shot FOAC and the Sequoia-800. By comparing the intensity of the main peak pulse and the sCMOS noise, a dynamic range of 10^{11} is obtained, which, to date, is the highest dynamic range observed for a single-shot TC measurement. In the experiment, to increase the intensity of the correlation signal, the sampling pulse is not expanded by the beam expander to keep its intensity in the overlapping area with the test pulse. As a result, the diameter is not as large as in the above first experiment and the time window is only about 50 ps. Interestingly, the ghost prepulse “a” introduced by the postpulse “A” measured by the Sequoia-800 is not detected by the FOAC again. To be mentioned, the intensity of postpulse “A” introduced by the 1-mm glass plate is measured to be about 0.5×10^{-3} at 10.5 ps. The second postpulse at 21 ps is measured to be about 3.2×10^{-7} , which is in good agreement with the calculated value about 2.5×10^{-7} . The intensity of the second postpulse is too weak to be observed.

As well as for increasing the correlation signal intensity and improving the detector sensitivity, suppressing the scattering noise is also important for a high dynamic range measurement of 10^{11} . Because the sampling pulse has the same central wavelength as the test pulse in the single-shot FOAC, the correlation signal obtained by SFM has the same central wavelength as the SHG signals of both the sampling and test pulses. Then the noise introduced by the SHG signals of the sampling and test pulses, which cannot be blocked by a spectral filter, needs to be analyzed. It is well known that the SHG process is a second-order optical parametric process that is sensitive to the phase-matching condition. Then a special cutting angle of the BBO

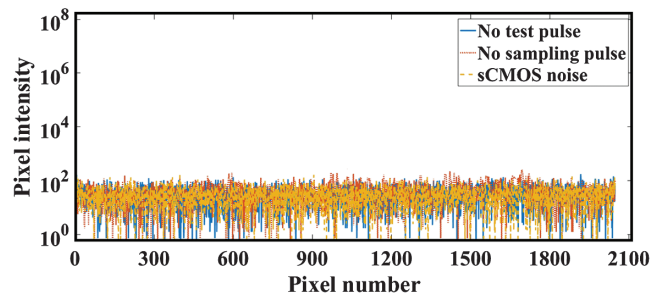


Fig. 8 The detector noise from the sCMOS and scattering noise from the SHG signals.

is designed to weaken the SHG generation. In the experiment, the crossing angles of the test and sampling pulses with respect to the optic axis of the BBO crystal are 99 deg and 61 deg, respectively, which are very different from the best phase-matching angle, i.e., 29.2 deg. This simple design makes the SHG scattering noise in this single-shot FOAC negligible. In the experiment, while blocking either the sampling pulse or test pulse, the intensity of the other SHG scattering noise is captured by the sCMOS camera. The sCMOS background noise is also obtained by covering the shutter of the sCMOS. The results are shown in Fig. 8 with different types of lines. The scattering noises from the SHG signals of both incident pulses are at the same scale as the background noise of the sCMOS camera. The results clearly prove the capability of 10^{11} dynamic range measurement using our single-shot FOAC system.

Finally, the single-shot FOAC is tested using a high TC laser pulse sampled from a PW laser pulse system.³² The sample pulses have a pulse energy of 10 mJ, a repetition rate of 1 Hz, a pulse duration of 40 fs, and a central wavelength of 800 nm. Two strip-shaped filters are included to reduce the main peak correlation signal in the experiment. The attenuation ratio of the filter is so large that only the main pulse can be observed and the information near the main pulse is lost, which would miss dynamic ratio data within 5-ps time window around the main pulse. In the future, we will try to solve this problem by fabricating a step variable density filter. Figure 9(a) shows the original data obtained by the single-shot FOAC. To make the weak signal more visible, the range of the color bar is adjusted to between 100 and 200. The signal is shown in Fig. 9(b). The TC curves of the sample pulse measured by the single-shot FOAC and Sequoia-800 are presented in Fig. 9(c). It can be seen that the two measurements in the time window from -40 to 10 ps are quite consistent with each other. A single-shot TC measurement of a PW laser system with a dynamic range of about 2×10^{10} and a time resolution of about 160 fs is obtained, which also shows the capability of the 10^{11} dynamic range. The correlation signal intensity is dependent on the intensities of the two incident pulses in the nonlinear crystal. The intensity profile of the two input beams on the BBO crystal is important for measurement accuracy of the dynamic range. It should be noted that the beam profile of the SD signal for sampling pulse after the third-order nonlinear process is uniform around the focused plane (the surface of the BBO crystal). Since the test pulse is picked out from the edge of the laser beam, the intensity distribution across the beam will not be uniform. The relatively weaker beam focused from the edge part will induce a weakened SFG signal, which may be the reason

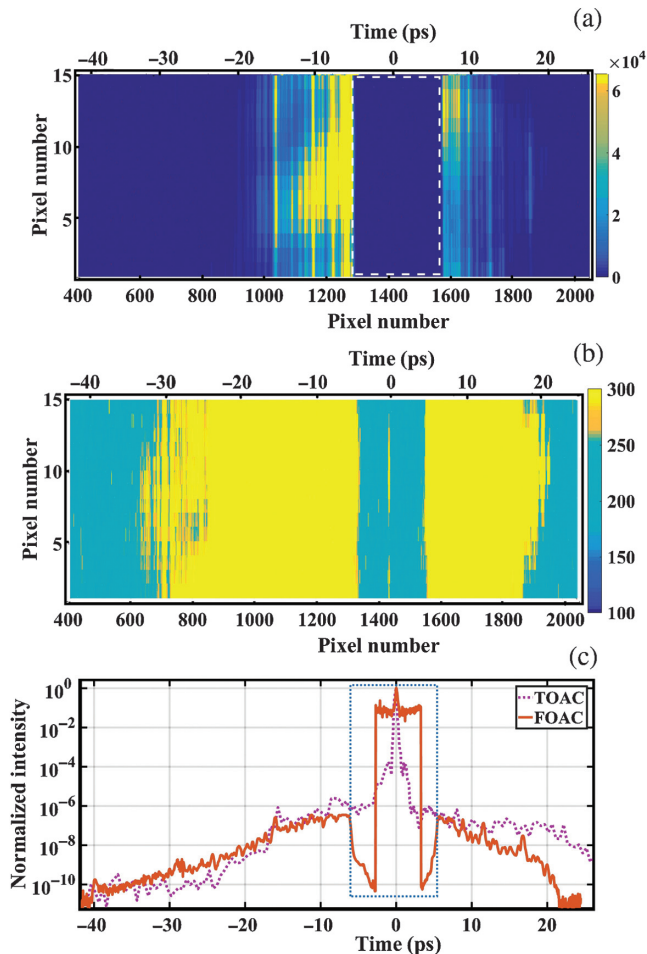


Fig. 9 The measurement results of the single-shot FOAC and delay-scanning TOAC (Sequoia-800). (a) The correlation signals on the sCMOS detector. (b) The correlation signals on the sCMOS detector when the range of the color bar is adjusted to make the weak signal more visible. (c) The comparison of the TOAC and FOAC measurement results. The strip-shaped density filters are used in the region of the dashed-line rectangle.

why there is large difference between the TOAC and FOAC for the data beyond 10 ps. Unfortunately, we did not measure the beam profile of the test beam on the BBO crystal this time. We expect to monitor the beam profiles of the two input beams on the SFG nonlinear crystal using CCD cameras in the future. Then, their intensity distributions will be used to correct the final results.

6 Conclusion

We have proposed a simple fourth-order autocorrelation method for single-shot TC measurement with higher time resolution and better fidelity than typical third-order autocorrelation or cross correlation methods. A single-shot FOAC is developed based on the SD process to generate clean sampling pulses. The proof-of-principle experimental results show a dynamic range of $\sim 10^{11}$, a time resolution of ~ 160 fs, and a time window of 65 ps capabilities of this single-shot FOAC. Higher dynamic ranges can be obtained in the future by increasing the thickness of the SFM crystal and improving the sensitivity of the detector.

A higher time resolution or a wider time window can be achieved using a magnified or reduced $4f$ mapping setup in front of the camera. The method and the corresponding single-shot FOAC device will benefit the improvement of PW laser systems and many important ultrahigh intense laser–matter interaction research activities such as the generation and acceleration of protons and ions, laboratory astronomy, fast-ignition inertial confinement fusion, and the generation of secondary sources of high-intensity γ rays.

Acknowledgments

This work was supported by the National Natural Science Foundation of China (NSFC) (Nos. 61527821 and 61521093), the Instrument Developing Project (No. YZZ201538), the Strategic Priority Research Program (No. XDB160106) of the Chinese Academy of Sciences (CAS), and Shanghai Municipal Science and Technology Major Project (No. 2017SHZDZX02). The authors would like to thank Dr. Xiaoming Lu, Dr. Xinliang Wang, and Dr. Lingang Zhang for providing the intense laser sources for the single-shot FOAC measurement.

References

1. D. Strickland and G. Mourou, “Compression of amplified chirped optical pulses,” *Opt. Commun.* **56**(3), 219–221 (1985).
2. A. Dubietis, G. Jonusauskas, and A. Piskarskas, “Powerful femto-second pulse generation by chirped and stretched pulse parametric amplification in BBO crystal,” *Opt. Commun.* **88**(4–6), 437–440 (1992).
3. C. Danson et al., “Petawatt class lasers worldwide,” *High Power Laser Sci. Eng.* **3**, e3 (2015).
4. W. Li et al., “339 J high-energy Ti:sapphire chirped-pulse amplifier for 10 PW laser facility,” *Opt. Lett.* **43**(22), 5681–5684 (2018).
5. B. Shen et al., “Exploring vacuum birefringence based on a 100 PW laser and an x-ray free electron laser beam,” *Plasma Phys. Controlled Fusion* **60**, 0444002 (2018).
6. Z. Guo et al., “Improvement of the focusing ability by double deformable mirrors for 10-PW-level Ti: sapphire chirped pulse amplification laser system,” *Opt. Express* **26**(20), 26776–26786 (2018).
7. H. Daido, M. Nishiuchi, and A. S. Pirozhkov, “Review of laser-driven ion sources and their applications,” *Rep. Prog. Phys.* **75**, 056401 (2012).
8. D. Batani et al., “Effects of laser prepulses on laser-induced proton generation,” *New J. Phys.* **12**, 045018 (2010).
9. O. Lundh et al., “Influence of shock waves on laser-driven proton acceleration,” *Phys. Rev. E* **76**, 026404 (2007).
10. M. Kaluza et al., “Influence of the laser prepulse on proton acceleration in thin-foil experiments,” *Phys. Rev. Lett.* **93**, 045003 (2004).
11. A. G. MacPhee et al., “Limitation on prepulse level for cone-guided fast-ignition inertial confinement fusion,” *Phys. Rev. Lett.* **104**, 055002 (2010).
12. H.-B. Cai et al., “Prepulse effects on the generation of high energy electrons in fast ignition scheme,” *Phys. Plasmas* **17**, 023106 (2010).
13. H. Kiriyama et al., “High-contrast high-intensity repetitive petawatt laser,” *Opt. Lett.* **43**(11), 2595–2598 (2018).
14. J. Wang et al., “In-band noise filtering via spatio-spectral coupling,” *Laser Photonics Rev.* **12**(8), 1700316 (2018).
15. C. Thaury et al., “Plasma mirrors for ultrahigh-intensity optics,” *Nat. Phys.* **3**, 424–429 (2007).
16. A. Jullien et al., “ 10^{-10} temporal contrast for femtosecond ultraintense lasers by cross-polarized wave generation,” *Opt. Lett.* **30**(8), 920–922 (2005).

17. S. Luan et al., "High dynamic range third-order correlation measurement of picosecond laser pulse shapes," *Meas. Sci. Technol.* **4**(12), 1426–1429 (1993).
18. C. Dorrer, J. Bromage, and J. D. Zuegel, "High-dynamic-range single-shot cross-correlator based on an optical pulse replicator," *Opt. Express* **16**(18), 13534–13544 (2008).
19. Y. Wang et al., "Single-shot measurement of $>10^{10}$ pulse contrast for ultra-high peak-power lasers," *Sci. Rep.-UK* **4**, 3818 (2014).
20. T. Oksenhendler et al., "High dynamic, high resolution and wide range single shot temporal pulse contrast measurement," *Opt. Express* **25**(11), 12588–12600 (2017).
21. L. Obst et al., "On-shot characterization of single plasma mirror temporal contrast improvement," *Plasma Phys. Controlled Fusion* **60**, 054007 (2018).
22. D. Haffa et al., "Temporally resolved intensity contouring (TRIC) for characterization of the absolute spatio-temporal intensity distribution of a relativistic, femtosecond laser pulse," *Sci. Rep.-UK* **9**, 7697 (2019).
23. X. Shen et al., "Temporal contrast reduction techniques for high dynamic-range temporal contrast measurement," *Opt. Express* **27**(8), 10586–10601 (2019).
24. A. Jullien et al., "Highly efficient temporal cleaner for femtosecond pulses based on cross-polarized wave generation in a dual crystal scheme," *Appl. Phys. B* **84**(3), 409–414 (2006).
25. X. Shen et al., "Linear angular dispersion compensation of cleaned self-diffraction light with a single prism," *High Power Laser Sci. Eng.* **6**, e23 (2018).
26. J. Liu et al., "Temporal contrast enhancement of femtosecond pulses by a self-diffraction process in a bulk Kerr medium," *Opt. Express* **18**(21), 22245–22254 (2010).
27. J. Liu et al., "Transient-grating self-referenced spectral interferometry for infrared femtosecond pulse characterization," *Opt. Lett.* **37**(23), 4829–4831 (2012).
28. V. A. Schanz et al., "Noise reduction in third order cross-correlation by angle optimization of the interacting beams," *Opt. Express* **25**(8), 9252–9261 (2017).
29. J. Collier et al., "A single-shot third-order autocorrelator for pulse contrast and pulse shape measurements," *Laser Part Beams* **19**(2), 231–235 (2001).
30. L. P. Yu et al., "High-contrast front end based on cascaded XPWG and femtosecond OPA for 10-PW-level Ti:sapphire laser," *Opt. Express* **26**(3), 2625–2633 (2018).
31. N. Xie et al., "Suppression of prepulses by a temporal pulse cleaner based on a self-diffraction process for an ultraintense femtosecond laser," *Optik* **178**, 279–284 (2019).
32. Y. Chu et al., "High-energy large-aperture Ti:sapphire amplifier for 5 PW laser pulses," *Opt. Lett.* **40**(21), 5011–5014 (2015).

Peng Wang received his BS degree from Xidian University in 2012 and his PhD from Shanghai Institute of Optics and Fine Mechanics (SIOM), Chinese Academy of Sciences, in 2017. Currently, he is an assistant researcher at SIOM. His research interests include four-wave mixing and temporal contrast measurement of laser pulses.

Xiong Shen received his BS degree from Tianjin University in 2012 and his PhD from Shanghai Institute of Optics and Fine Mechanics (SIOM), Chinese Academy of Sciences, in 2018. Currently, he is an assistant researcher at SIOM. His research interests include femtosecond laser pulse measurement.

Jun Liu is a professor of Shanghai Institute of Optics and Fine Mechanics (SIOM), Chinese Academy of Sciences. He received his PhD from SIOM in 2007. He conducted his postdoctoral research at the University of Electro-Communications (Japan) from 2007 to 2010, and was promoted to the role of assistant professor in 2010. Since 2011, he has been working at SIOM. His research interests include femtosecond laser technology, light sheet microscopy, optical imaging through scattering media, and photodynamic therapy.

Ruxin Li is director and professor of Shanghai Institute of Optics and Fine Mechanics (SIOM), Chinese Academy of Sciences. He received his PhD from SIOM in 1995, and conducted his postdoctoral research at Uppsala University (Sweden) and at the University of Tokyo (Japan) from 1996 to 1998. Since 1998, he has been working at SIOM. His research is known for development of petawatt lasers, laser wakefield acceleration, high order harmonic generation, and femtosecond laser filamentation.